JOURNAL OF MATERIALS SCIENCE 37 (2002) 4589–4595

The preparation and properties of iron base self-fluxing alloy spray-welding coatings with different rare earths and chromium content

Y. L. CHENG*
Department of Chemistry, Zhejiang University, Hangzhou 310027, People's Republic of China; Department of Inorganic Materials, Sichuan University, Chengdu 610065, People's Republic of China
E-mail: deepblacksea@163.com

C. Q. ZHENG
Department of Inorganic Materials, Sichuan University, Chengdu 610065, People's Republic of China

Z. ZHANG, F. H. CAO, J. F. LI
Department of Chemistry, Zhejiang University, Hangzhou 310027, People's Republic of China

J. Q. ZHANG
Department of Chemistry, Zhejiang University, Hangzhou 310027, People's Republic of China; State Key Laboratory for Corrosion and Protection, Shenyang 110015, People's Republic of China

J. M. WANG
Department of Chemistry, Zhejiang University, Hangzhou 310027, People's Republic of China

This investigation studied the effects of rare earths (RE) and chromium on the high temperature oxidation resistance and aqueous corrosion resistance of iron base self-fluxing alloy coatings. Four coatings were prepared through smelting-atomizing and oxide-acetylene flame spraying. The properties of the coatings were evaluated by cyclic oxidation tests, weight loss experiments, electrochemical impedance spectroscopy (EIS), potentiodynamic scanning technique, scanning electron microscopy (SEM) and electron dispersive X-ray analysis (EDAX). The addition of RE greatly enhanced the oxidation resistance of the coatings. This effect was attributed to the fact that RE changed the ion diffusion patterns of the coatings in the process of scale forming, resulting in more protective scales with high adhesion. The increase of chromium content in the coatings enhanced the corrosion resistance of the coatings in nitric acid solution, but in hydrochloric acid and sulfuric acid solutions the result was reversed. Rare earth addition had a beneficial effect in sulfuric acid and nitric solutions, but in hydrochloric acid, the samples with RE had a corrosion rate slightly higher than that of the samples without RE addition. These results are explained by the effect that the addition of RE minimized the cathodic area of the coatings. © *2002 Kluwer Academic Publishers*

1. Introduction

Self-fluxing alloys are a group of important materials used in thermal spraying. Thermal spraying includes a group of techniques such as HVOF (High Velocity Oxygen Fuel spraying), flame spraying, plasma spraying, and filament-arc spraying. It can produce specific surface properties and almost all the materials that have stable molten phases can be processed. So far, more and more attention has been paid to this technique [1, 2], and it is obvious that the materials used in thermal spraying play a decisive role on the properties of thermal spray coatings. Nowadays, a group of materials widely used are iron base, nickel base, and cobalt base self-fluxing alloys. The iron base self-fluxing alloy possesses excellent wear resistance and a relatively cheap price, but its poor high temperature oxidation and aqueous corrosion resistance restrict its applications. The nickel and cobalt base self-fluxing alloys have excellent overall properties, but they are too expensive. If the properties of iron base alloy were enhanced, the nickel and cobalt alloys would be replaced by iron base alloys to some extent. RE are called the "vitamin" of metals, which means that a small amount of RE can greatly enhance the properties of metals [3–5]. For the above reasons,

*Author to whom all correspondence should be addressed.

studies on the application of RE in spray-welding materials have increased since 1990. However, there are only a few studies on the effects of RE on the microstructure and wear resistance of the spray-welding alloy coatings in the literature, effects of RE on the oxidation resistance and corrosion resistance have not been widely reported yet [6]. In this study, iron base self-fluxing spray-welding coatings with different amounts of RE and chromium were prepared, and their high temperature oxidation and corrosion resistances were investigated by cyclic oxidation tests, weight loss experiments, electrochemical impedance spectroscopy (EIS), and potentiodynamic scanning technique.

2. Experimemtal details

2.1. Preparation of different iron base self-fluxing alloy spray-welding coatings

To prepare the iron base self-fluxing alloy spray-welding coatings, four kinds of alloys were prepared by melting the raw materials in an intermediate frequency inductive coreless electric furnace according to the composition listed in Table I, the amount of the RE added in the alloys was based on the study of Yi [6].

After the alloy was molten, it was atomized by high-pressure nitrogen gas (RE were added just before the atomization of the molten alloys). After atomization, the powders of the alloy were sieved to the needed granularity. Then the coatings were prepared by the oxide-acetylene flame spray-welding technique. lastly, coatings were cut to make samples with the dimension of $20 \times 10 \times 5$ mm to undergo the following high temperature oxidation and aqueous corrosion tests.

The RE used in this study was the mixed rare earths alloy with a composition of Ce 47, La 26, Nd 18 and Pr 5 wt%.

2.2. High temperature cyclic oxidation tests

To simulate the working condition of high temperature alloys, the cyclic oxidation experimental method (GB/13303) [7] was used to evaluate the oxidation resistance of the coatings. The samples of coatings were polished and all the edges were eliminated. Before testing, the samples were degreased in alcohol and dried. The oxidation temperature was 1000°C and the time for every oxidation cycle was 20 hours. After each cycle, the samples were cooled to room temperature, stored in desiccators and weighted. Every sample experienced six cycles.

2.3. Aqueous corrosion tests

To evaluate the aqueous corrosion properties of the coatings, the conventional weight loss experiments (GB10124-88) [8], potentiodynamic scanning measurements, and EIS (electrochemical impedance spectroscopy) measurements have been conducted.

Tests were carried out in 3.0 wt%HCl, 10.0 wt% H_2SO_4 and 10.0 wt%HNO_3solutions. The solutions were prepared by analytical reagents and deionized water. All the experiments were conducted at room temperature (25°C).

The test time for the weight loss tests was 24 hours, after each of the tests, the corrosion products on the samples were cleaned and the weight loss measured; then the corrosion rates of the samples were calculated.

For the EIS and potentiodynamic measurements, the samples were connected to a copper wire, and enveloped by epoxy with only one face of about 0.5 cm^2 exposed as a working surface; the working surfaces were polished with diamond paste. The testing system was the conventional 3-electrode electrochemical cell, the reference electrode was a saturated calomel electrode (SCE), and a large platinum foil served as the auxiliary electrode. The EIS measurements were performed at the corrosion potential with a Solatron1280 electrochemical measurement unit. The frequency range of the measurement in this study is 0.005 Hz–20000 Hz. The measurements were always taken in the direction of decreasing frequency, and the amplitude of the sinusoidal signal was 5 mV. All the EIS measurements were carried out after 30 min immersion of the samples in the corrosive media. Potentiodynamic scanning measurements were performed with a Solatron SI1287 electrochemical interface.

TABLE I The composition of four kinds of iron base self-fluxing alloys prepared (wt%)

Group of alloys	Cr	Ni	B	Si	C	Fe	RE
Cr18	18.0	12	2.5	3.5	0.3	Balance	None
Cr25	25.0	12	2.5	3.5	0.3	Balance	None
Cr18RE	18.0	12	2.5	3.5	0.3	Balance	0.2
Cr25RE	25.0	12	2.5	3.5	0.3	Balance	0.2

3. Results and discussions

3.1. High temperature oxidation experiments

Fig. 1 shows the relationships between the weight increase of samples and oxidation time From Fig. 1, it can be seen that after 3 cycles (60 hr), the weight increases of the four iron base self-fluxing alloy coatings are similar, but after 3 cycles, the difference become quite distinctive. The samples with rare earth addition (Cr18RE, Cr25RE) show a low weight increase, but the samples without RE addition (Cr18, Cr25) show a rapid weight increase. The surfaces of oxidized samples were

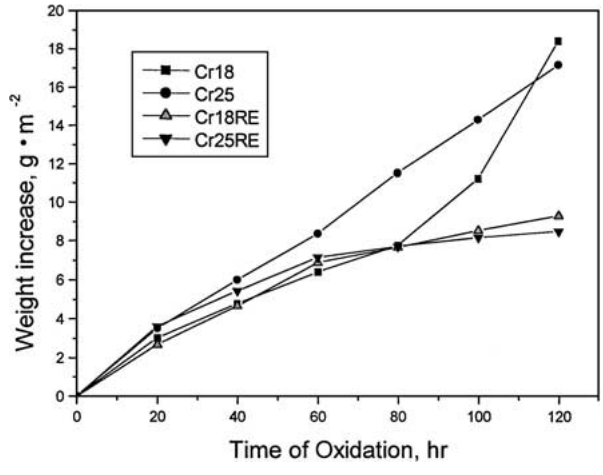

Figure 1 Relationship between the weight increase of samples and time of oxidation.

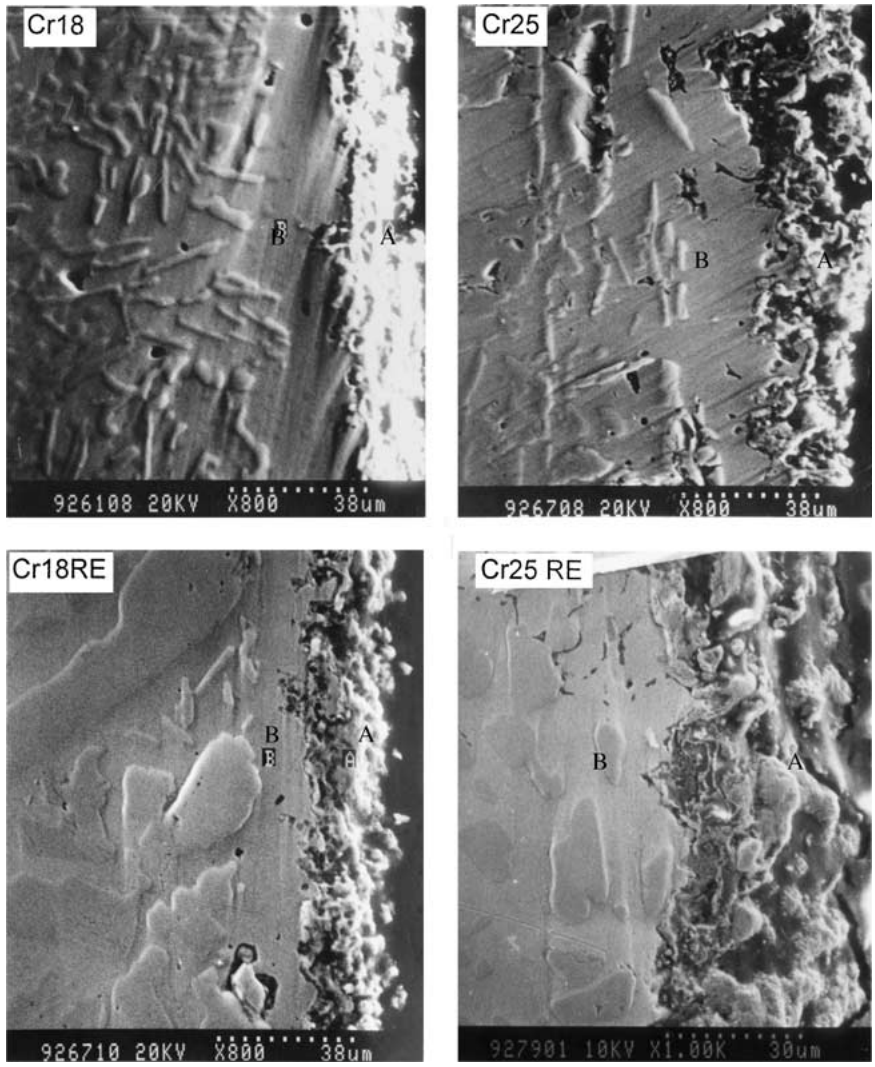

Figure 2 The SEM images of the scales of four kinds of samples.

observed during the experiment, and it was found that the scales of samples with RE addition kept intact after 6 cycles, but the scales of samples without RE addition suffered serious cracking and spallation.

To be protective to oxidation, an oxide scale must possess good adherence, a high melting point, a low vapor pressure, good high temperature plasticity to resist fracture, and low electrical conductivity, or low diffusion coefficients for metal ions and oxygen. For cyclic temperatures the metal and oxide should possess similar coefficients of expansion [9]. If the scale of the metal easily cracked and spalled, it would be nonprotective, which is the case for samples Cr18, Cr25 in this experiment. In the case of samples with RE addition (Cr18RE, Cr25RE), the scales kept intact during oxidation tests, which can protect the samples from further oxidation, and explains why the weight increase of Cr18RE and Cr25RE were much less than that of Cr18, Cr25 after 6 cyclic oxidations.

The reason why the addition of rare earth greatly enhanced the oxidation resistance of iron base self-fluxing alloy spray-welding coatings can undoubtedly be attributed to the high adhesion of the scales of samples Cr18RE and Cr25RE. But the mechanism of this effect is disputable, and many mechanisms have been proposed [10], a commonly accepted one being that the pegs of rare earth oxide extend from the metal into the scale and key it to the metal surface [11].

The SEM images of the cross section of the scales of the four kinds of iron base self-fluxing coatings are shown in Fig. 2. Table II is the EDAX result of Fig. 2.

The morphologies of the scales of the four samples are quite different in Fig. 2, especially the scale of sampleCr18 and its substrate have quite different features, which indicate that their structure and properties must be quite different, and which may explain why the scale of sample Cr18 is easy to crack. It can also be seen that the scales of Cr18, Cr25 are quite porous, but the scales of Cr18RE, Cr25RE are compact, especially the scale of Cr25RE which is the most compact.

According to the studies of Graham, the mass transportation process of high temperature oxidation of Fe-Cr alloys is dominated by the outward diffusion of Cr^{3+} cations; the contribution of the inward transportation of oxygen is only 1% [12]. Therefore, it is reasonable to speculate that the scales of Cr18, Cr25 are formed at the interface of oxygen and oxide. Under the high temperature condition of this experiment, the outward diffusion of cations is very rapid, resulting in the condensation of voids at the interface of the alloy and scale. Therefore, a porous scale will be formed, whose structure must have a large difference of coefficient of

TABLE II The element distribution between the oxidized layer and substrate of the samples in Fig. 2

	A (scale) (wt%)						B (substrate) (wt%)			
Sample	Cr	Fe	Ni	Si	Ce	O	Cr	Fe	Ni	Si
Cr18	51.76	8.33	0.59	5.47	0.00	33.86	4.72	78.72	13.50	3.51
Cr25	47.45	9.40	1.96	6.88	0.00	34.31	8.41	67.45	18.73	5.40
Cr18RE	39.54	12.31	2.67	9.78	0.28	35.45	8.83	69.44	16.40	5.33
Cr25RE	42.91	17.47	3.40	3.49	0.42	32.31	15.06	67.14	14.67	3.13

expansion between the oxide and metal, and the scale easily cracks and spalls when the samples are cooled.

However, in the cases of Cr18RE and Cr25RE, due to the addition of RE, the mechanism of scale formation is probably changed. The rare earth can promote the anionic diffusion rather than the cationic diffusion [10], which can avoid the void formation at the interface between scale and metal as in the case of sample Cr18 and Cr25. The reason why the scales of Cr18RE and Cr25RE are more compact is probably due to this effect. The RE are a group of reactive elements, and their atomic radii are moderately large, which make their atoms mostly form rare earth oxide and segregate easily to grain boundaries. In the case of high temperature oxidation, the grain boundaries are the important short-circuit paths for mass diffusion [13] and the RE on the grain boundary must block this path, which will result in reduced outward cation diffusion, thus the oxygen inward diffusion becomes dominant. EDAX analysis confirms the above speculation: the Cr fraction under the scales of the samples with rare earth addition (Cr18RE, Cr25RE) is much grater than that of the corresponding samples (Cr18, Cr25), this apparently shows the slow Cr^{3+} outward diffusion of the samples with RE (At the B site in Fig. 2, which is right under the scales, the chromium content of Cr18 is 4.72%, but Cr18RE is 8.83%, Cr25 is 8.41%, while Cr25RE is 15.06%).

3.2. Aqueous corrosion tests

The results of the weight loss experiments are shown in Figs 3–5.

During the immersion tests of the four kinds of coatings in 3.0 wt%HCl and 10.0 wt%H_2SO_4 solution, hydrogen evolution was obviously observed. But in the 10.0 wt% HNO_3 solution, the four kinds of coatings behaved differently, hydrogen bubbles were only observed on the surface of the samples with lower chromium content (sample Cr18, Cr18RE). Meanwhile, a more important phenomenon was observed that, after the immersion test of all the four kinds of samples in nitric solution, the color of the electrolyte became brown, which showed that the corrosion mechanism for the samples in nitric solution is different from the mechanism in hydrochloric acid and sulfuric acid.

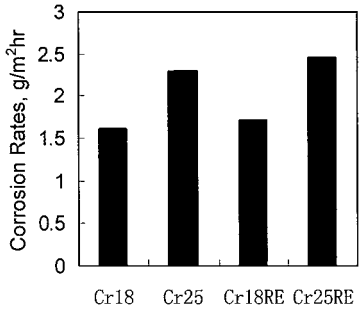

Figure 3 Corrosion Rates in 3 wt%HCl solution.

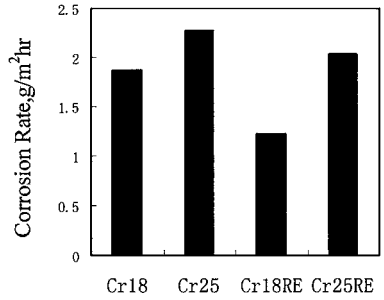

Figure 4 Corrosion Rates in 10 wt% H_2SO_4 solution.

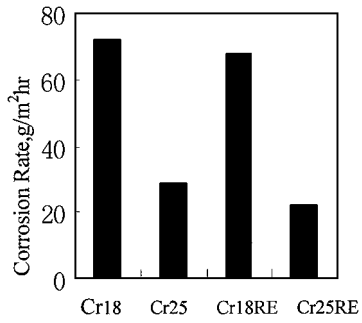

Figure 5 Corrosion Rates in 10.0 wt%HNO_3 solution.

As shown in Figs 3–5, the corrosion rates in 10.0wt% HNO_3 solution were the largest. In different corrosive media, the corrosion rates ranked as below: in 3.0 wt%HCl solution, Cr25RE > Cr25 > Cr18RE > Cr18; in 10.0 wt% H_2SO_4 solution, Cr25 > Cr25RE > Cr18 > Cr18RE; and in 10.0 wt% HNO_3 solution, Cr18 > Cr18RE > Cr25 > Cr25RE.

In the weight loss tests, we found that the corrosion product was somewhat difficult to clean, which would bring error to the testing results. To compensate for this, EIS and potentiodynamic scanning method have also been conducted.

Figs 6 and 7 show the results of the EIS measurements of the samples in 3.0 wt%HCl and 10.0 wt% HNO_3 solutions respectively the frequency range of the EIS measurements was 20000 Hz-0.005 Hz.

In Figs 6 and 7, the high frequency part of the Nyquist plots of the samples consist of only one semi-circle; this part of all the Nyquist plots can be fitted by the equivalent circuit in Fig. 8.

In Fig. 8, R_s is the solution resistance, R_p is the resistance of the corrosion reaction, which can be related to the corrosion resistance of the samples in the corrosive media, while the CPE in Fig. 8 is the so called constant

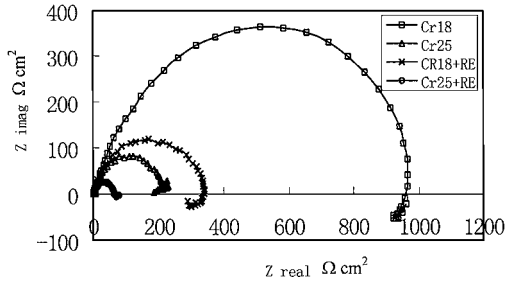

Figure 6 Nyquist plots of the four kinds of self-fluxing alloy coatings in 3 wt%HCl solution.

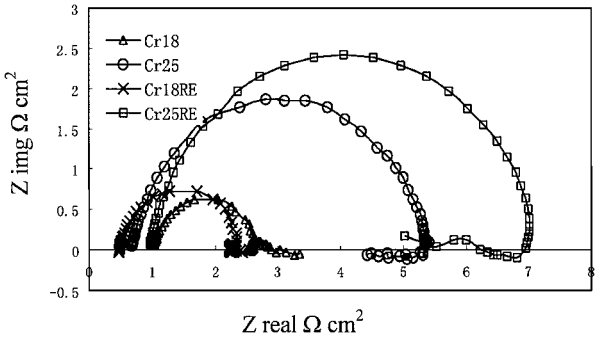

Figure 7 Nyquist plots for the four kinds of iron base self-fluxing alloy coatings in 10 wt% HNO_3 solution.

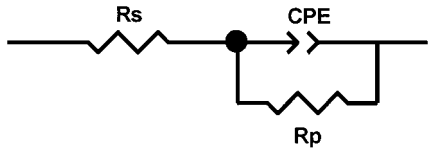

Figure 8 The equivalent circuit for the high frequency part of the Nyquist plots in Fig. 6 and 7.

phase angle element, which is expressed as an exponent affecting the imaginery component of a complex impedance.

$$Z_{\mathrm{CPE}} = \frac{1}{Y_0(j\omega)^n} \tag{1}$$

For $n = 1$ represents an ideal capacitance with $C = Y_0$; $n = 0$ a resistance with $R = 1/Y_0$; $n = 0.5$, a warburg; and $n = -1$ an inductance with $L = 1/Y_0$. The presence of a CPE often has been explained by dispersion effects that can be caused by microscopic roughness of a surface [14–16], local discrepancies in the coating thickness or the high resistance of the surfacce layers.

Tables III and IV list the values for equivalent elements of the Nyquist plots in Figs 6 and 7 respectively.

Fig. 9 represents the potentiodynamic scanning (PDS) curves of the samples in 3.0 wt% HCl solution at

TABLE III Equivalent values for the Nyquist plots in 3 wt% HCl solution

Samples	R_s (Ω cm^2)	R_p (Ω cm^2)	CPE/Y0 (Ω^{-1} cm^{-2})	CPE/n
Cr18	1.39	1001.00	1.79E-4	0.80444
Cr25	0.89	212.23	2.29E-4	0.84601
Cr18RE	0.66	337.46	2.61E-4	0.79353
Cr25RE	1.10	62.85	3.81E-4	0.86882

TABLE IV Equivalent values for the Nyquist plots in 10 wt% HNO_3 solution

Samples	R_s (Ω cm^2)	R_p (Ω cm^2)	CPE/Y0 (Ω^{-1} cm^{-2})	CPE/n
Cr18	1.01	1.70	0.00501	0.81174
Cr25	0.67	4.76	0.00292	0.83839
Cr18RE	0.48	1.95	0.00358	0.83264
Cr25RE	0.94	6.25	0.00188	0.84106

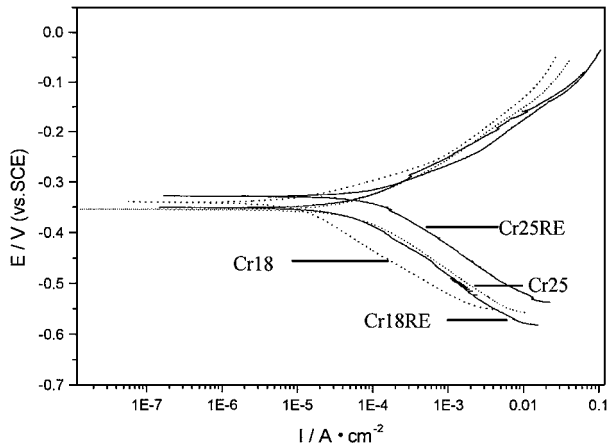

Figure 9 The potentiodynamic scanning curves of the four kinds of iron base self-fluxing alloy coatings in 3 wt% HCl solution.

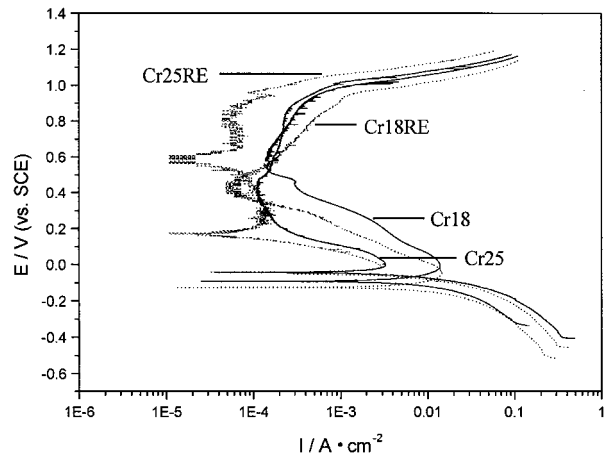

Figure 10 The potentiodynamic scanning curves of the four kinds of iron base self-fluxing alloy coatings in 10 wt%HNO_3 solution.

a sweep rate of 0.2 mV/s, between −0.2 V from open circuit potential (OCP) and 0.3 V from OCP. Fig. 10 represents the PDS curves of the samples in 10 wt% HNO3 solution at a sweep rate of 0.5 mV/s, between −0.4V from OCP and 1.25 V from OCP.

It can be seen from the PDS curves that the four kinds of coatings show passivity in the HNO_3 solutions. The samples with higher chromium contents show higher corrosion potentials and their passivity currents are less than that of the samples with low chromium contents, but in HCl solution, none of the samples show passive properties.

Tables V and VI show the analyzed results of the PDS curves in Figs 9 and 10 respectively. Where R_p, I_o and E_o are the polarization resistance, corrosion current and corrosion potential respectively.

TABLE V The values of parameters of the PDS curves in 3.0 wt%HCl (Fig. 9)

Samples	R_p (Ωcm^2)	I_o (A cm^{-2})	E_o
Cr18	1183.3	1.1914E-5	−0.0994
Cr25	264.98	3.7466E-5	−0.1130
Cr18RE	321.48	5.6926E-5	−0.1095
Cr25RE	125.8	1.4547E-4	−0.0875

TABLE VI The values of parameters of the PDS curves in 10.0 wt%HNO_3 (Fig. 10)

Samples	R_p (Ω cm^2)	I_o (A cm^{-2})	E_o
Cr18	3.21	0.00813	−0.0922
Cr25	4.81	0.00543	−0.0415
Cr18RE	2.14	0.0121	−0.1276
Cr25RE	6.88	0.00379	−0.0420

It can be seen that R_p values acquired from the EIS measurements and the R_p values acquired from the potentiodynamic measurements are very close. Polarization resistance is calculated as the inverse of the slope of the I vs E graph near the open circuit potential. The higher the value of R_p is, the higher the corrosion resistance of the material.

The polarization resistance (R_p) of the four samples is ranked as Cr18 > Cr18RE > Cr25 > Cr25RE in 3 wt% HCl solution, and Cr25RE > Cr25 > Cr18RE > Cr18 in 10 wt% HNO_3 solution. Because R_p value is a reflection of the corrosion resistance of the samples, those orders are consistent with the results of the weight loss tests. We can see for the evaluation of the corrosion resistance of the samples, the weight loss experiment, EIS and potentiodynamic scanning measurements all can correctly predict the corrosion resistance of samples, but the EIS is quickest and non-damaging (due to its very small potential applied).

From the result of the above experiments, conclusions about the effects of RE and chromium content can be summarized as follows:

The chromium content can deteriorate the corrosion resistance of iron base self-fluxing alloy coatings in H_2SO_4 and HCl solution, but can enhance the corrosion resistance of the coatings in nitric acid. This is consistent with the reports in the literature: in the 1920–1930s, the study of the chromium containing steels were focused on its corrosion resistance in sulfuric acid, this resulted in the false conclusion that chromium deteriorates the corrosion resistance of alloys [17]. The reason is that the chromium content can result in the passivity of the alloy, but when the alloy has not reach the

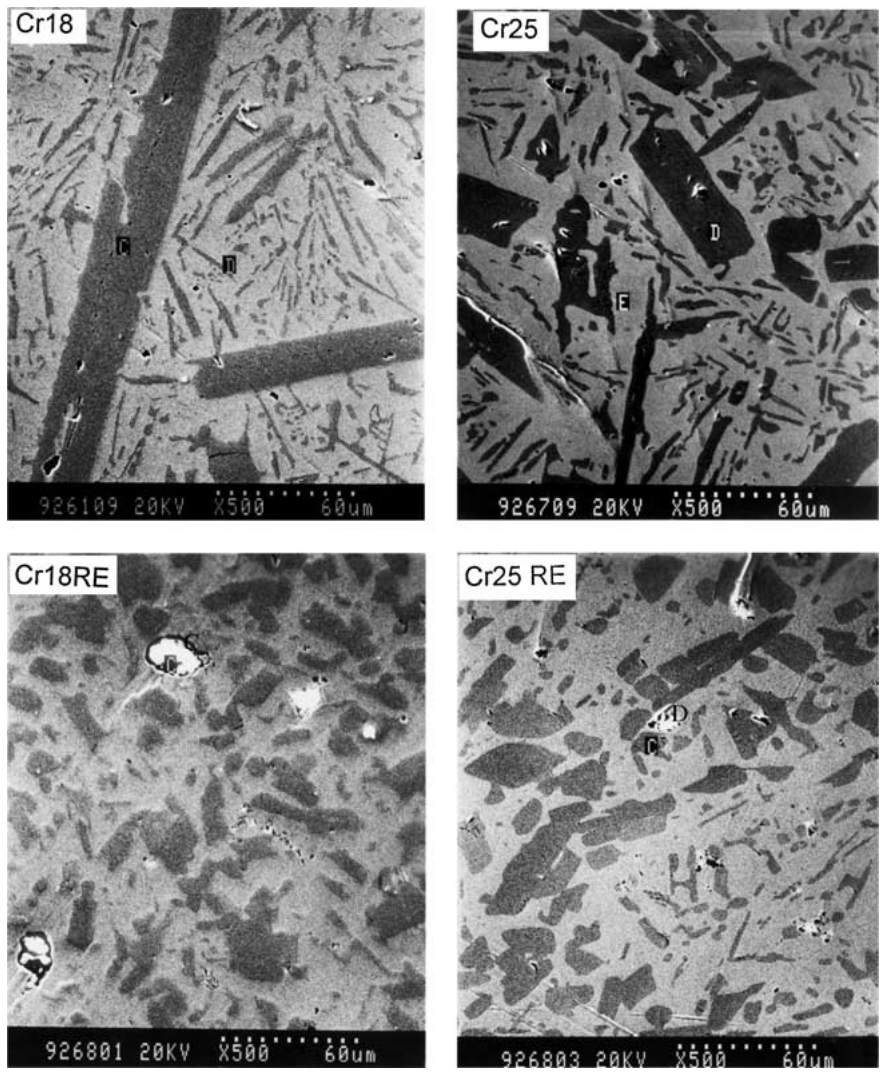

Figure 11 SEM images of the four kinds of iron base self-fluxing alloy coatings.

TABLE VII EDAX analysis of the two phases of coatings Cr18 and Cr25 (wt%)

	Cr	Fe	Ni	Si
Matrix of Cr18	5.93	71.21	17.66	5.20
Second phase of Cr18	46.17	52.21	1.41	0.21
Matrix of Cr25	7.42	67.42	19.81	5.50
Second phase of Cr25	56.74	41.98	0.98	0.30

passive state, the corrosion rate will increase with the chromium content.

In sulfuric and nitric acid, rare earth addition has a beneficial effect, but in the hydrochloric acid, the samples with RE have corrosion rates slightly higher than those of the samples without RE addition.

To analyze the behavior of these experimental results, the microstructure of the coatings has been analyzed by SEM. Fig.11 is the SEM images of these coatings.

It can be seen in Fig. 11 that the coatings mainly consist of two phases. One phase is the matrix, with a light color; the second phase is the phase with a darker color. The composition of the two phases of Cr18 and Cr25 has been analyzed by EDAX. The results are shown in Table VII. According to the EDAX results and the Fe-Cr-Ni ternary phase diagram, it can be concluded that the matrix may has a structure of austenite while the second phase may has a structure of ferrite. They will behave differently in solutions this will be discussed later.

Corrosion reactions can be divided into anodic reactions and cathodic reactions, which most likely take place on the different sites on the surface of the samples. In the corrosion resistance tests of these samples, the most likely cathodic reaction in the hydrochloric acid and sulfuric acid is hydrogen evolution. But in the nitric acid, the reaction of NO_3^- depolarization plays an important role: $NO_3^- + 2H^+ + e = NO_2 + H_2O$, and this explains why the corrosion rates in nitric acid are the largest. The result of EDAX analysis shows that the second phase of the coatings has a very high chromium content. Due to the strong passivity effect caused by Cr content, the second phase may act as sites for the cathodic reaction, and the matrix act as the site of metal ions dissolution. This phenomenon is similar to the intergranular corrosion of stainless steels in which the chromium depletion region of the grain boundary dissolved in advance. In SEM images of these samples (see Fig. 11), we can see that the microstructure of the coatings was changed by the addition of RE. The second phase of the coatings with RE addition is very fine, it has apparent distinction with the large rod shaped second phase of the coatings without RE, which shows that the RE addition can suppress the forming of the second phase, resulting a smaller cathodic area of the samples. That the RE addition can refine the grain of metals and suppress the forming of second phase has observed by many authors and was explained by the segregation of the large radius RE atom on the phase boundaries [18]. In the sulfuric corrosion test, the corrosion reaction is under cathodic control, and the coatings with RE will have a lower corrosion rate. But in hydrochloric acid, due to the effects of Cl^-, the corrosion reaction is under the anodic control, the effect of a smaller cathode area will increase the corrosion current. This is consistent with the phenomenon we observed in this study.

4. Conclusions

1. The addition of RE can greatly enhance the high temperature oxidation resistance of the iron base self-fluxing spray-welding coatings. The mechanism of this effect is probably that the RE promotes preferential anionic diffusion, resulting in a more protective scale that can resist the thermal stress.

2. Coatings with high chromium content have better corrosion resistance in 10.0 wt% nitric solution, but it is the reverse in 3.0 wt% hydrochloric acid and 10.0 wt% sulfuric acid solution.

3. The addition of RE can enhance the corrosion resistance of the coatings in 10 wt% sulfuric acid, and 10 wt% nitric acid solution, but degrade the corrosion resistance of the coatings in 3 wt% hydrochloric solution. The mechanism is that the addition of RE can reduce the cathodic area in the coatings.

Acknowledgments

The authors wish to acknowledge the financial support of the National Natural Science Foundation of China (Approval No.50071054), the Special Funds of the China Major State Basic Research Project (G19990650) and the financial support of the State Key Laboratory for Corrosion and Protection (China). The authors also gratefully thank Mrs. J.F. Xu for her invaluable help in finishing this article.

References

1. R. W. SMITH and R. KNIGHT, *JOM*. August (1995) 32.
2. S. SAMPATH and H. HERMAN, "Thermal spray technology," ASM, Material Park, OH (1988) 1.
3. J. ZHANG, J. Z. ZHAO, J. S. E and H. X. DANG, *J. RE* **9**(4) (1991) 285.
4. P. DUCROS, *J. Less Common Metals* **111** (1985) 37.
5. N. E. RYAN, in "RE Resources-Science, Technology and Applications," edited by R. G. Bautista and N. Jackson (TMS, 1991) p. 389.
6. W. YI, C. Q. ZHENG, P. FAN, S. H. CHEN, W. LI and G. F. YIN, *Journal of Alloys and Compounds* **311** (2000) 65.
7. The National Standard GB/13303-91 of the People's Republic of China, 1991.
8. The National Standard GB10124-88 of the People's Republic of China, 1988.
9. M. G. FONTANA, in "Corrosion Engineering," 3rd edn. (McGraw-Hill, 1986) p. 506.
10. L. V. RAMANATHAN, *Corrosion Prevention & Control* (June 1998) 87.
11. B. LUSTMAN, *Trans. AIME* **88** (1950) 995.
12. M. J. GRAHAM, *Corrosion Science* **37** (1995) 1377.
13. G. M. ECER and G. H. MEIER, *Oxid. Metals*. **13** (1979) 159.
14. Z. ZHANG, J. Q. ZHANG, J. M. WANG and C. N. CAO, *Trans. Nonferrous Met. Soc China* **11** (2001) 284.
15. C. J. URCHURTU, *Corrosion* **47** (1991) 472.
16. C. J. URUCHURTU and J. L. DAWSON, *ibid*. **43** (1987) 19.
17. J. M. XIAO, in "Pandect of Corrosion—Corrosion of Materials and Method of Control" (Chemical Industry, Beijing, 1994) p. 192.
18. MUQIN LI, CHEN MA and DECHUN SHAO, *Journal of the Chinese Rare Earth Society* 14 (1994) 163.

Received 13 November 2001
and accepted 22 May 2002